Development, Characterization, and Application of a Cadmium-Selective Microelectrode for the Measurement of Cadmium Fluxes in Roots of *Thlaspi* Species and Wheat[1]

Miguel A. Piñeros, Jon E. Shaff, and Leon V. Kochian*

United States Plant, Soil, and Nutrition Laboratory, United States Department of Agriculture-Agricultural Research Service, Cornell University, Ithaca, New York 14853

A Cd^{2+}-selective vibrating microelectrode was constructed using a neutral carrier-based Cd ionophore to investigate ion-transport processes along the roots of wheat (*Triticum aestivum* L.) and two species of *Thlaspi*, one a Zn/Cd hyperaccumulator and the other a related nonaccumulator. In simple $Cd(NO_3)_2$ solutions, the electrode exhibited a Nernstian response in solutions with Cd^{2+} activities as low as 50 nM. Addition of Ca^{2+} to the calibration solutions did not influence the slope of the calibration curve but reduced the detection limit to a solution activity of 1 μM Cd^{2+}. Addition of high concentrations of K^+ and Mg^{2+} to the calibration solution to mimic the ionic composition of the cytoplasm affected neither the slope nor the sensitivity of the electrode, demonstrating the pH-insensitive electrode's potential for intracellular investigations. The electrode was assayed for selectivity and was shown to be at least 1000 times more selective for Cd^{2+} than for any of those potentially interfering ions tested. Flux measurements along the roots of the two *Thlaspi* species showed no differences in the pattern or the magnitude of Cd^{2+} uptake within the time frame considered. The Cd^{2+}-selective microelectrode will permit detailed investigations of heavy-metal ion transport in plant roots, especially in the area of phytoremediation.

Advances in the technologies and methodologies for studying ion transport in higher plant cells have advanced our understanding of the mechanisms by which plants absorb ions from soils and translocate them into the shoots. These advances can be used to increase our understanding of the phytoremediation of metal-contaminated soils. Phytoremediation is a "green technology" with which terrestrial plants are used as an inexpensive, low-technology method to remediate surface soils contaminated with toxic heavy metals. A number of plant species have been identified that are endemic to metalliferous soils and can tolerate and accumulate high levels of heavy metals such as Zn, Cd, Pb, Cu, and Ni in the shoot (Brooks et al., 1977; Baker et al., 1994). These plants, called hyperaccumulators, can grow in soils contaminated with high levels of heavy metals by translocating and accumulating high concentrations in the shoots. For example, *Thlaspi caerulescens*, a Zn/Cd hyperaccumulator, can grow in soils containing concentrations as high as 35 μM Cd and 1830 μM Zn (Brown et al., 1994) and can accumulate up to 40,000 μg g^{-1} Zn in its shoots (Chaney, 1993). By comparison, the normal foliar Zn concentration for hydroponically grown plants is approximately 100 to 200 μg g^{-1} and 30 μg g^{-1} is considered adequate. This species also accumulates high levels of Cd in its tissues. These unique aspects of the physiology of *T. caerulescens* make it an ideal candidate for the study of the mechanisms by which such hyperaccumulator plants can tolerate and accumulate toxic levels of heavy-metal ions. Recent studies have started to reveal some of the fundamental mechanisms by which these plants accumulate heavy metals in shoots (Lasat et al., 1996). Still, there is little known about the fundamental biology concerning plant mechanisms of shoot heavy-metal hyperaccumulation.

Several techniques have been used to obtain estimates and to characterize fluxes of macro- and micronutrient ions in higher plant cells. Intact tissue techniques have often relied on bulk-solution methods, such as radioisotope-flux methods or solution-depletion measurements (Cataldo et al., 1983; Mullins and Sommers, 1986). Such approaches integrate ion uptake over the entire tissue surface, providing an averaged measurement over a period of time. Because these types of techniques are constrained in terms of the spatial and temporal resolution, they are usually used to study ion uptake into entire roots or root systems over fairly long periods. In recent years technological advances have facilitated the fabrication of liquid-membrane ISEs for a number of ions, which has made it possible to map ion-activity gradients (i.e. ion-transport processes) in the unstirred layer along the root surface. Diffusion analysis of these steady-state gradients has, for example, allowed researchers to calculate net K^+, H^+, and Ca^{2+} fluxes associated with localized regions of the root surface of maize (*Zea mays* L.) (Newman et al., 1987; Kochian et al., 1989; Ryan et al., 1990), as well as NH_4^+ and NO_3^- fluxes in barley roots (Henriksen et al., 1990, 1992; McClure et al., 1990), and the effects of other ions (e.g. Al^{3+}) on various ion-transport systems in wheat roots (Miyasaka et al., 1989; Huang et al., 1992b; Ryan et al., 1992).

Abbreviations: ISE, ion-selective microelectrode; MPM, matched potential method; mV/dec, millivolts per decade change in ion activity; SSM, separate solution method.

More recently, the development of a vibrating ISE system has proven to be a substantial improvement over the static ISE described above (Smith et al., 1994). By way of comparison, the sensitivity of the static liquid-membrane ISE is limited by the voltage drift due to the inherent high resistance (10^{10} Ω) of these electrodes, such that ion fluxes can be measured only as long as the background concentration is kept below approximately 0.3 mM. Likewise, smaller fluxes, such as Ca^{2+} influx into mature regions of the root, are very hard to detect, even at low background concentrations. Kühtreiber and Jaffe (1990) overcame these system limitations by developing a vibrating Ca^{2+}-selective microelectrode that exhibited a greatly improved sensitivity over static electrodes. It allowed them to measure small extracellular Ca^{2+} gradients associated with Ca^{2+} fluxes in single cells such as fucoid eggs, pollen tubes, and moving amoebae. Vibrating ion-selective electrodes have subsequently been used to characterize root ion-transport processes with a high degree of spatial and temporal resolution (Huang et al., 1992a; Ryan and Kochian, 1993; Jones et al., 1995). Kochian et al. (1992) conducted a detailed comparison of static and vibrating ISE techniques to quantify K^+, H^+, and Ca^{2+} transport in intact maize roots and suspension cells. This study showed that the vibrating electrodes were approximately 50 times more sensitive than static microelectrodes, making vibrating electrodes the technique of choice when studying root-ion fluxes of small magnitude or ion-transport processes in single cells.

In the present work we have taken advantage of the vibrating-electrode technology, along with the synthesis of a Cd^{2+} ionophore (Schneider et al., 1980), to develop and characterize a Cd^{2+}-selective electrode and to demonstrate its potential in studying Cd^{2+} transport in roots of nonaccumulator and hyperaccumulator plant species.

MATERIALS AND METHODS

Construction of Cd^{2+}-Selective Microelectrodes

The construction of liquid-membrane ISEs has been previously described in detail (Lucas and Kochian, 1986; Kühtreiber and Jaffe, 1990; Smith et al., 1994). Borosilicate glass capillaries (1.5 mm in diameter, without filament, catalog no. TW150–4, World Precision Instruments, Inc., Sarasota, FL) were cleaned in a mixture of 95% (v/v) concentrated H_2SO_4 and 5% (v/v) of 70% $HClO_4$. Capillaries were pulled using a two-stage Flaming-Brown horizontal electrode puller (model P-87, Sutter Instrument Co., Novato, CA), generating a microelectrode with a relatively short shank and a tip diameter of approximately 1 to 2 μm. Microelectrodes were heated (200°C, $\geq$ 3 h), silanized with tri(n-butyl)chlorosilane (200°C, 30 min), cooled, and then stored in an evacuated desiccator. Microelectrodes were back filled completely with an electrolyte buffer (10 mM Cd[NO$_3$]$_2$ plus 100 μM KCl). The microelectrode tip was then front filled with a short column (50 μm in length) of Cd^{2+} sensor, which consisted of 10% (w/w) Cd^{2+} ionophore I (N,N,N',N'-tetrabutyl-3,6-dioxaoctanedi[thioamide]; ETH1062 catalog no. 20909, Fluka), 10% (w/w) potassium tetrakis(3,5 bis-[trifluromethyl]phenyl)borate (catalog no. 60588, Fluka), and 80% (w/w) 2-nitrophenyl octyl ether (catalog no. 73732, Fluka). Subsequently, the back-filling buffer was reduced to a column length of approximately 1.5 cm to minimize parasitic capacitance. Electrical contact between the microelectrode and the head stage of the vibrating probe system was made through a 0.25-mm Ag: AgCl$_2$ wire, and a single-junction reference electrode (model MI-409F, Microelectrodes, Inc., Londonderry, NH) was connected to the reference input of the head stage.

Vibrating-Microelectrode System

A detailed description of the technique, the theoretical aspects of the device, and the calculations involved in the ion-selective system have been previously described (Kühtreiber and Jaffe, 1990; Kochian et al., 1992; Smith et al., 1994). The system consists of three piezoelectric microstages (PZS-100; Burleigh Instruments, Inc., Fishers, NY) stacked in orthogonal directions and held by translation stages (Newport Corp., Fountain Valley, CA). The stepper motors of the translation stages allow coarse positioning of the microelectrode, and the piezoelectric pushers control the electrode's vibration. The piezoelectric pushers are driven by a damped, squared wave at low frequency (0.3 Hz), vibrating the microelectrode at any desired angle and amplitude in a two-dimensional plane.

The system was mounted on the stage of an inverted microscope (IM 35, Zeiss) equipped with a video camera. A 486-PC computer running DVIS6 software (Biocurrents Research Center, Marine Biology Lab, Woods Hole, MA) controlled the movement of the microelectrode between the two preset positions (i.e. vibration amplitude) such that the excursion of the electrode was damped. Generally, the vibration amplitude is set at 30 μm for most experiments but can be shortened for smaller voltage gradients. The software also allows for the visual display of the voltage difference, which is calculated by measuring the microelectrode output at each extreme position of the vibration excursion (1000 data points/s), pooling these data into two separate buffers representing the two extremes of vibration, and then subtracting the averaged data of one buffer from the other. The sensitivity of the system permits the measurement of voltage differences in the microvolt range. These voltage gradients are translated into the ion-activity gradient by using the calibration curve of the microelectrode, which relates the voltage output of the microelectrode to specific ion activities in solution.

Selectivity Measurements

The ability of the Cd^{2+} electrode to discriminate against other ions was evaluated using two methods. Since preliminary work on selectivity suggested that the Cd^{2+} electrode was highly discriminatory against other cations, we used two novel techniques. The first approach (Bakker, 1996, 1997a, 1997b) involved evaluating the electrode's performance in the absence of Cd^{2+}, the primary ion. The electrode was first back filled with the cation salt of the tetraphenyl borate derivative used in making the Cd^{2+} sensor

(in this case K^+ as 100 mM KCl) and then the electrode was front filled with the Cd^{2+} sensor as described above. The liquid membrane was then conditioned for several hours in a solution identical to the back-filling solution. Calibration curves for the individual interfering ions were generated by measuring the electrode millivolt outputs in a series of solutions of varying activities of the interfering ion. Only after these calibration curves were generated for the interfering ions was the electrode exposed to the primary ion (Cd^{2+}) and a similar calibration curve was then generated for varying Cd^{2+} activities. The selectivity coefficients were then calculated using the general formula:

$$\log K_{IJ}^{pot} = \frac{z_j F\{E_i - E_j\}}{2.303\, RT} + \log[a_j/a_i^{z_j/z_i}]$$

where I and J represent the interfering and primary ions, respectively. K_{IJ}^{pot} is the selectivity coefficient, z_i and z_j are the valences of the interfering and primary ions tested, E_j and E_i are the electrode millivolt outputs in the testing solutions, a is the activity of the interfering and primary ion, R is the gas constant, F is the Faraday constant, and T is the absolute temperature.

The second approach used the MPM (Gadzekpo and Christian, 1984; Umezawa et al., 1995), which is the method of choice for calculating selectivity coefficients when the electrode does not exhibit a Nernstian response to changes in interfering ion activity. This method involved adding a specific activity of the primary ion, Cd^{2+}, to a reference solution already containing a defined Cd^{2+} activity and then measuring the millivolt output. In a separate test, interfering ions were added to an identical Cd^{2+} reference solution until the change in membrane potential matched the previous one obtained by adding primary ions (Cd^{2+}) to the reference solution. The matched potential selectivity coefficient was then calculated from the ratio of the activity of the primary ion to that of the interfering ion:

$$K_{IJ}^{MPM} = a_I/a_J$$

where I and J represent the interfering and primary ions, respectively, K_{IJ}^{MPM} is the selectivity coefficient, and a is the ion activity.

Ion Gradient Sources for Efficiency Determination

A Cd^{2+} source, which was used to generate a standing Cd^{2+} gradient to test the efficiency of the vibrating Cd^{2+}-selective microelectrode system, was constructed by filling a blunt-tipped microelectrode (tip diameter approximately 10 μm) with a solution of 99.9 mM $Cd(NO_3)_2$ and 0.1 mM $Mg(NO_3)_2$ in 0.5% (w/v) agarose. The agarose was included in the filling medium to minimize bulk water movement into the source. This source was placed in a Petri dish containing 0.1 mM $Cd(NO_3)_2$ and 99.9 mM $Mg(NO_3)_2$ and was allowed to equilibrate overnight. Theoretical values for the Cd^{2+} gradient generated at the tip of this source were calculated according to the following equation:

$$\Delta V = S[(-U\Delta r)/(C_b r^2 + Ur)]/2.3$$

where ΔV is the change in millivolts over the vibration excursion of the electrode, S is the slope of the electrode calibration, r is the distance from the source, Δr is the amplitude of vibration, C_b is the background concentration of Cd^{2+}, and U is an empirical constant. Empirical measurements were achieved by vibrating the electrode through a small amplitude (10 μm) at a frequency previously determined to be the most efficient in detecting the gradient (0.3 Hz). Calculation of U was achieved by first generating a calibration curve to characterize the electrode response and then taking a series of static millivolt readings (measuring Cd^{2+} activity) at known distances from the source. The millivolt readings were then converted to Cd^{2+} activity values using the calibration curve. A plot of these activity values (C) versus the inverse of the distance from the Cd^{2+} source ($1/r$) yields a line with a slope of U, according to the equation:

$$C = C_b + U/r.$$

Measurement of Ion Fluxes

Ion fluxes were calculated using Fick's first law of diffusion:

$$J_{Cd} = D_{Cd}(C_1 - C_2)/\Delta X$$

where J is the net Cd^{2+} flux (in picomoles per square centimeter per second), D_{Cd} is the diffusion constant for Cd^{2+} (7.2×10^{-6} cm^{-2} s^{-1} [Parsons, 1959]), C_1 and C_2 are the Cd^{2+} activities at the two extremes of vibration (in micromolar per cubic centimeter), and ΔX is the amplitude of vibration (in centimeters).

For the transport studies, root seedlings were set in a plastic Petri dish containing 50 μM $Ca(NO_3)_2$ solution, and the primary root (for wheat [*Triticum aestivum* L. cv Grandin]) or a single root from the root system (for the two *Thlaspi* spp.) was anchored to the bottom of the dish with notched Plexiglas blocks that straddled the root and were attached to the dish bottom with silicone grease. For wheat, this solution was exchanged with a solution consisting of 50 μM $Ca(NO_3)_2$ plus 5 μM $Cd(NO_3)_2$ 10 min before starting the flux measurements. For *Thlaspi caerulescens* and *Thlaspi arvense* seedlings we found it necessary to allow the plant to be exposed overnight to the 50 μM $Ca(NO_3)_2$ plus 5 μM $Cd(NO_3)_2$ solution to detect significant Cd^{2+} fluxes. Flux measurements were carried out at different positions along the root. Microelectrodes were vibrated perpendicularly to the root with an amplitude of 30 μm such that the extremes of the vibration were between 30 and 60 μm from the root surface. Experiments were performed at 22°C ± 2°C. Ionic activities were calculated using the GEOCHEM PC program (Parker et al., 1995).

Plant Material

Seeds of wheat were obtained from the North Central Research Center (Minot, ND). Seeds of *T. caerulescens*, a Zn/Cd hyperaccumulator (originally collected from a Zn/Cd smelter site in Prayon, Belgium), were generously provided by Dr. Alan Baker (University of Sheffield, UK),

and seeds of *T. arvense*, a related nonaccumulator, were obtained from the Crucifer Genetic Cooperative (catalog no. CrGC 16–1, University of Wisconsin, Madison). Wheat seeds were surface sterilized in 0.5% NaOCl for 15 min and then germinated in the dark for 2 d on filter paper saturated with 0.2 mM $CaSO_4$. Germinated seeds were transferred to polyethylene cups with mesh bottoms, covered with black polyethylene beads, and then placed into the precut holes of the covers of black polyethylene containers, which held 2.4 L of aerated 0.2 mM $CaSO_4$ solution. Plants were grown for an additional 2 d before being used for the flux studies. The primary root length of the intact 4-d-old seedlings was about 10 cm.

T. caerulescens and *T. arvense* seeds were placed in a drop of 0.7% (w/v) low-temperature-gelling agarose, which sat on nylon mesh circles (1-mm mesh openings) and, in turn, were positioned on a coarser mesh support covering a 5-L black plastic tub. The nylon mesh was covered with black polyethylene beads. Seeds were germinated for 5 d in the dark in deionized water. Subsequently, deionized water was replaced with a nutrient solution containing the following macronutrients (in mM): Ca, 0.8; K, 1.2; Mg, 0.2; NH_4, 0.1; NO_3, 2.0; PO_4, 0.1; and SO_4, 0.2; and micronutrients (in μM): BO_3, 12.5; Cl, 50; Cu, 0.5; Fe-*N,N'*-ethylenebis(2-[2-hydroxyphenyl]-Gly), 10.0; MoO_4, 0.1; Mn, 1.0; Ni, 0.1; and Zn, 1.0. The solution was buffered at pH 5.5 with 1 mM Mes-Tris. Seedlings were grown in a growth chamber at 25/15°C (light:dark, 16:8 h) under a light intensity of 300 μmol photons m^{-2} s^{-1}. Plants were grown for 2 to 3 weeks before being used for the flux studies. The length of the whole root system was about 5 to 10 cm.

RESULTS

Calibration of the Cd^{2+}-Selective Microelectrode

The calibration for the Cd^{2+}-selective microelectrodes over a wide range of solution Cd^{2+} activities is shown in Figure 1. The slope of the calibration curve (32 mV/dec) was close to that predicted theoretically (28.5 mV/dec) by the Nernst equation, indicating that the microelectrode was sensitive to Cd^{2+} over a wide range of Cd^{2+} activities (10^7-fold). In addition, the electrode showed a linear response over this range of activities, showing departure from linearity (i.e. loss of sensitivity) at activities lower than 50 nM Cd^{2+}.

Because a defined Ca^{2+} activity in the uptake solution is required for normal root growth and function, we evaluated the Cd^{2+}-electrode sensitivity with a constant Ca^{2+} background. The electrode response over a large range of Cd^{2+} activities with a constant Ca^{2+} background is shown in Figure 2. At the two Ca^{2+} background concentrations tested (50 and 200 μM Ca^{2+}), the sensitivity of the electrode for Cd^{2+} (29 and 27 mV/dec, respectively), was close to that predicted theoretically (28.5 mV) by the Nernst equation. The electrode maintained a high Cd^{2+} sensitivity over a 10^5-fold range of Cd^{2+} activities in the presence of 50 and 200 μM Ca^{2+}. The electrode showed a linear Nernstian response down to Cd^{2+} activities as low as 1 μM. We also
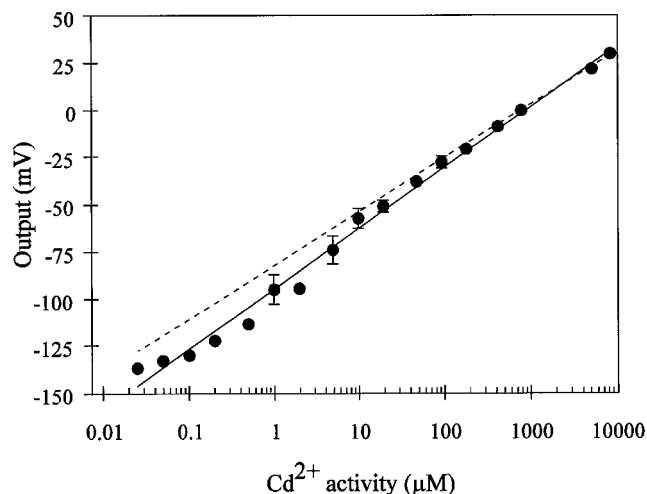

Figure 1. Calibration curve for the Cd^{2+} microelectrode in $Cd(NO_3)_2$ solutions varying in activity. The electrode's output was arbitrarily defined as 0 for the reading taken when its Cd^{2+} activity was 784 μM, which corresponds to a 1 mM $Cd(NO_3)_2$ solution. The output of electrode potential (relative to the potential of the reference electrode) for the different calibration solutions was then referred to this 0 level. The solid line is the linear regression for the experimental points. The sensitivity (slope) is equal to 32 mV/dec (r^2 = 0.992). The dotted line represents the Cd^{2+} electrode's ideal Nernstian change in potential for an electrode that is selective only for Cd^{2+}. SES are shown when they are bigger than the symbol. Data points represent the average responses of four different electrodes.

assessed the ability of the electrode to measure Cd^{2+} activities under conditions approximating the cell cytoplasm and vacuole, where the activities of potentially interfering background cations are high. Thus, we tested the sensitivity of the electrode in an artificial cytoplasm containing 100 mM K^+ and 2 mM Mg^{2+}. The sensitivity of the electrode under these conditions is shown in Figure 3. The slope of the calibration curve (29 mV/dec) is close to that predicted theoretically (28.5 mV/dec) by the Nernst equation. Thus, the electrode remains highly sensitive and selective for Cd^{2+} under conditions that mimic the plant cell cytoplasm. Below Cd^{2+} solution activities of 1 μM, the electrode response was still linear but exhibited sub-Nernstian behavior (19 mV/dec between 50 nM and 1 μM Cd^{2+} concentrations).

Ion Selectivity

Further tests were conducted to assess the selectivity of the electrode for Cd^{2+} over other ions. We chose to consider eight divalent and three monovalent cations, which were either heavy metals (Pb^{2+}, Cu^{2+}, and Zn^{2+}) or would be part of our hydroponic growth medium (Fe^{2+}, Ni^{2+}, Mn^{2+}, Mg^{2+}, Ca^{2+}, Na^+, K^+, and NH_4^+). Prior to adopting more detailed methods for determining electrode selectivity (the MPM and the method of Bakker [1996]), we assessed the Cd^{2+} electrode's selectivity using the traditional SSM (Buck and Lindner, 1994). The SSM is based on determining the electrode's millivolt output first in a solution of 10 mM $Cd(NO_3)_2$, which yields the output E_{Cd}. Then, the

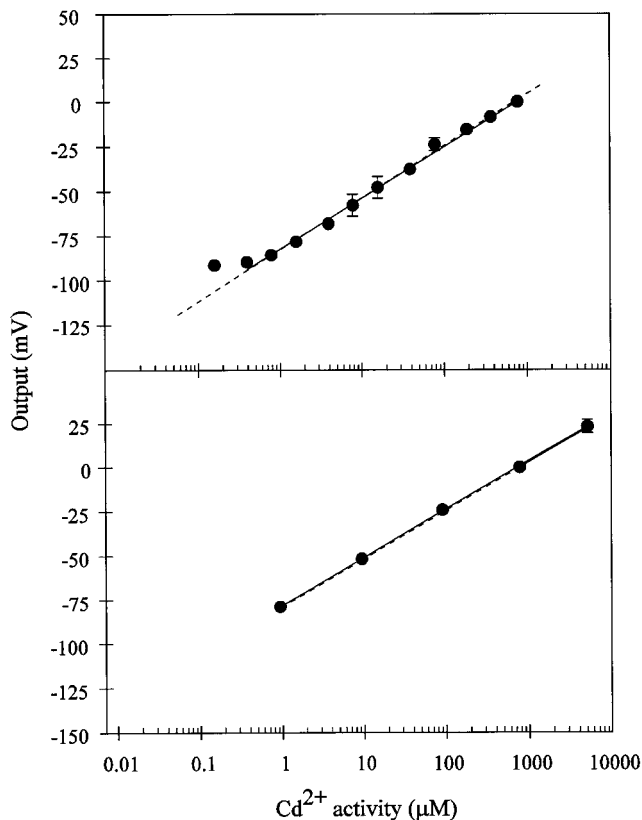**Figure 2.** Calibration curves for the Cd^{2+} microelectrode in $Cd(NO_3)_2$ solutions containing either 200 μM $Ca(SO_4)_2$ (top) or 50 μM $Ca(NO_3)_2$ (bottom). The electrode response (in millivolts) was arbitrarily defined as 0, as described in Figure 1. The solid line in both cases is the linear regression for the experimental points. The sensitivity (slope) is equal to 29 mV/dec ($r^2 = 0.995$ excluding the lowest point) for the calibration in 200 μM $Ca(SO_4)_2$ and 27 mV/dec ($r^2 = 0.999$) for the calibration in 50 μM $Ca(NO_3)_2$. SES are given if bigger than the symbol. Points represent, respectively, the averages of three and five different electrodes for the 200 μM $Ca(SO_4)_2$ (top) and 50 μM $Ca(NO_3)_2$ (bottom) background. The dashed line represents the theoretical change in potential for an electrode with ideal Cd^{2+} selectivity, as calculated by the Nernst equation.

electrode output is measured in a 10 mM solution of the interfering ion, which yields the output E_t. A selectivity value is then calculated from the difference of these two outputs, according to the Nicolsky-Eisenman equation (Buck and Lindner, 1994). We repeated the SSM in solutions in which the Cd^{2+} and interfering ion concentrations were 100 μM, which are more physiologically relevant. The selectivity coefficients calculated for each interfering ion with the SSM differed for the two concentrations used. The electrode was consistently more selective for Cd^{2+} over other ions when estimated in the 10 mM solutions (data not shown). This difference was most dramatic for the three monovalent cations tested: K^+, Na^+, and NH_4^+. This discrepancy in values is probably due to the non-Nernstian response of the electrode to these interfering ions at the two different activities used.

Based on this lack of consistency in the SSM technique we adopted two approaches to assess the selectivity of the

electrode. The first technique, the MPM, is prescribed for those electrode systems in which interfering ions and/or the primary ion do not satisfy Nernstian conditions (Umezawa et al., 1995). We used this technique because the lack of interference by K^+ and Mg^{2+} in the "artificial cytoplasm" and the minimal interference by Ca^{2+} suggested that the Cd^{2+} microelectrode was insensitive to a number of potentially interfering cations, and thus, these cations would display non-Nernstian responses. Using this technique we were able to calculate selectivity coefficients only for Cu^{2+} (0.0465) and for Pb^{2+} (0.27) ions. These values indicate that the Cd^{2+} electrode is 21 and 4 times more selective for Cd^{2+} than for Cu^{2+} and Pb^{2+}, respectively. Addition of any of the other interfering ions resulted in the reduction of the electrical output (data not shown). This reduction in potential could be accounted for by the dilution of the Cd^{2+} activity in the solution, suggesting that the interfering ions had no direct effect on the electrode.

A novel technique for measuring the Cd^{2+} electrode's true response to interfering cations, first proposed by Bakker (1996), was then used. The selectivity coefficients of the Cd^{2+} microelectrode obtained for eight divalent cations and for three monovalent cations using this technique are summarized in Table I. The convention for these selectivity coefficients is such that a log value of 0 indicates that the microelectrode cannot discriminate between the ion of interest, Cd^{2+}, and an interfering ion. Values less than 0 indicate that the microelectrode preferentially responds to the ion of interest over the interfering ion. Again, these results show that the microelectrode was highly selective for Cd^{2+} over other cations. From the selectivity coefficients presented in Table I, the electrode is between 800 and 10^{12} times more selective for Cd^{2+} over the other cations tested.
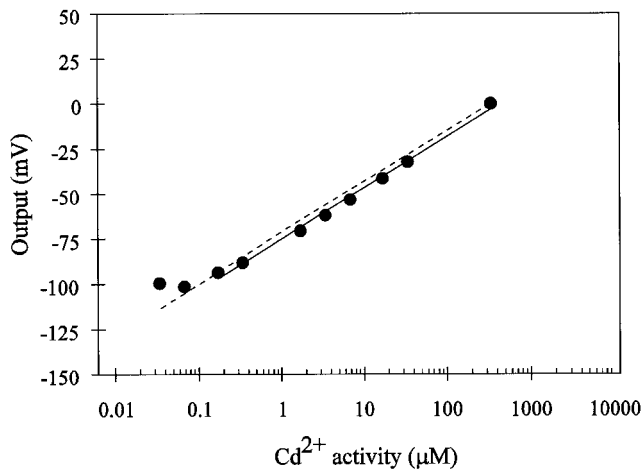

Figure 3. Calibration curve for the Cd^{2+} microelectrode in $Cd(NO_3)_2$ solutions containing a background of 100 mM KNO_3 and 2 mM $Mg(NO_3)_2$ (i.e. artificial cytoplasm). The electrode response (in millivolts) was arbitrarily defined as 0, as described in Figure 1. The solid line is the linear regression for the experimental points. The sensitivity (slope) is equal to 29 mV/dec ($r^2 = 0.995$ excluding the two lowest activity points). The dotted line represents the theoretically expected response for a Cd^{2+}-selective microelectrode with an ideal Cd^{2+} selectivity, as calculated by the Nernst equation.

Table I. *Selectivity coefficients for the Cd^{2+}-selective vibrating microelectrode*

Cd^{2+} microelectrodes were back filled with 100 mM KCl, front filled with Cd^{2+} sensor, and then conditioned in 100 mM KCl overnight. Calibration curves were generated for each of the cations listed below to demonstrate that the electrode had a Nernstian response for these interfering ions in the absence of Cd^{2+}. A calibration curve for Cd^{2+} was then generated. Selectivity coefficients were calculated from a general formula based on the Nicolsky-Eisenman equation (see "Materials and Methods").

Interfering Ion (J^{n+})	Log K_{KJ}^{pot}
Zn^{2+}	−2.9
Pb^{2+}	−4.6
Cu^{2+}	−4.8
Mn^{2+}	−5.2
Fe^{2+}	−8.6
Ni^{2+}	−10.4
Ca^{2+}	−10.8
Mg^{2+}	−12.2
NH_4^+	−6.2
Na^+	−7.1
K^+	−7.9

pH Effects on the Electrode

The response of the Cd^{2+} microelectrode to pH was tested to assess its utility in a variety of experimental situations. We evaluated the electrode's performance over a pH range spanning from 4.0 to 8.0, using buffers consisting of 10 mM Homopipes (homopiperazine-N-N'-bis-2-[ethanesulfonic acid]) and 10 mM Tris added in the appropriate proportions to achieve the desired pH. From Figure 4, it is evident that solution pH had no effect on the electrode's response to 50 μM Cd^{2+} in the buffered solution. The same response was observed in buffered solutions containing 10 μM Cd^{2+} (data not shown).

Efficiency Measurements

A micro-Cd^{2+} source was used to generate a Cd^{2+} activity gradient in solution, and then a series of static mil-
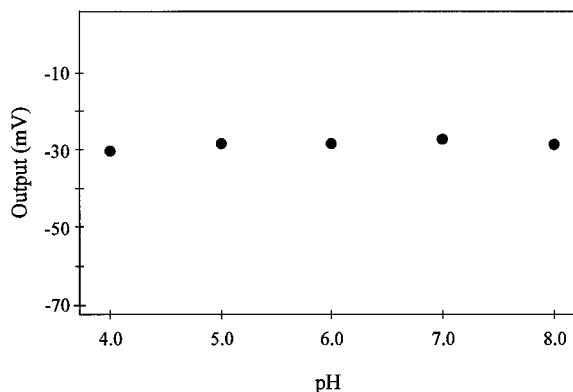
livolt readings were taken at different known distances from the gradient calibration source to characterize the gradient. Subsequently, the vibrating Cd^{2+} microelectrode was used to measure the same Cd^{2+} gradient (Fig. 5). This approach determines the efficiency of the vibrating Cd^{2+} microelectrode to detect a specific Cd^{2+} gradient. The experimentally measured Cd^{2+} gradient had a slope of −80.5 mV/cm between 0.004 and 0.01 cm from the source (b = 0.85 mV and r^2 = 0.941), in contrast to the theoretical value of −144.9 mV/cm (b = 1.56 mV and r^2 = 0.985) over the same range of distances. The ratio between the experimental and the theoretical slopes yielded a 55% efficiency for the vibrating Cd^{2+} microelectrode system. Thus, for our measurements of root Cd^{2+} fluxes, flux values had to be corrected to take into account that the vibrating Cd^{2+} microelectrode was only detecting approximately 55% of the gradient.

Measurement of Cd^{2+} Fluxes in Intact Root Systems

Because it was determined that the inclusion of Ca^{2+} in the bathing medium did not interfere with Cd^{2+} flux mea-
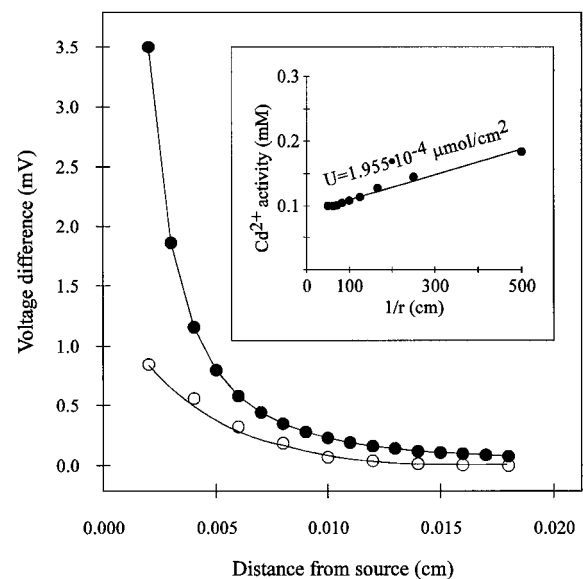

Figure 5. Theoretical (○) and experimental (●) measurements of a Cd^{2+} gradient as a function of distance from the artificial Cd^{2+} gradient source. Theoretical values were calculated according to the following equation: $\Delta V = S([-U\Delta r]/[C_b r^2 + Ur])/2.3$, where ΔV is the change in millivolts over the vibration excursion, S is the slope of the electrode, r is the distance from the source, Δr is the amplitude of vibration, C_b is the background activity of Cd^{2+}, and U is an empirical constant. Experimental measurements were made by vibrating the electrode through a 10-μm amplitude at different distances from the Cd^{2+} source. Inset, Calculation of the empirical constant, U. Static measurements were made at a series of distances from the source and then the millivolt outputs were converted to activity values. A plot of these activity (C) values versus the inverse of the distance from the Cd^{2+} source ($1/r$) yields a line with a slope of U, according to the equation: $C = C_b + U/r$, where C_b is the background activity of Cd^{2+} (0.09 mM), and U (in micromoles per square centimeter) defines the diffusion characteristics of the gradient source (r^2 = 0.992).

Figure 4. Effect of pH on Cd^{2+} microelectrode performance. The pH of five different 50 μM $Cd(NO_3)_2$ solutions were adjusted over a range spanning from pH 4.0 to 8.0, using a series of buffers consisting of 10 mM Homopipes and 10 mM Tris added in the appropriate proportions to achieve the desired pH. The electrical output of the electrode was measured and then referenced to a 0 level, as described in Figure 1.

surements, we were then able to measure Cd^{2+} fluxes along the intact roots of wheat and the two *Thlaspi* spp. Figure 6 shows a representative Cd^{2+} flux profile along a wheat root. Cd^{2+} influx at positions 1 to 1.5 mm from the root apex was significantly higher than that at positions further back from the apex. At the more distal positions (approximately 2 mm back from apex) the Cd^{2+} flux was much smaller and could vary between Cd^{2+} efflux and influx at different positions. This same profile was observed along roots of *T. caerulescens* and *T. arvense* (Fig. 7). It is interesting that there were no significant differences in the Cd^{2+} flux between the two *Thlaspi* spp. Additionally, although Cd^{2+} efflux was observed at positions 2 mm back from the wheat root apex (Fig. 6), no Cd^{2+} efflux was observed in either variety of *Thlaspi*, even at positions as far back as 18 mm from the root apex.

DISCUSSION

In the present work we have provided results that demonstrate the utility of an ion-selective Cd^{2+} microelectrode as a research tool to study heavy-metal transport in bio-
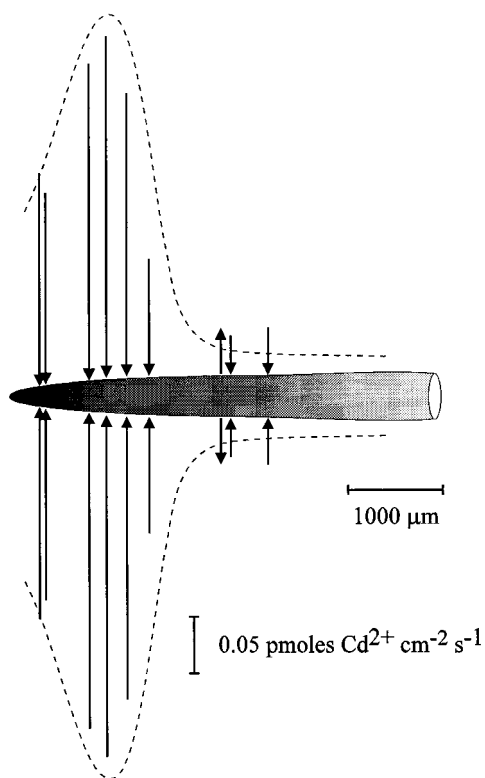

Figure 6. Diagram illustrating the Cd^{2+} flux profile along the longest seminal root of a 4-d-old wheat seedling. Flux measurements were carried out in 50 μM Ca(NO$_3$)$_2$ plus 5 μM Cd(NO$_3$)$_2$ at different positions along the root. The position and the magnitude of the fluxes are indicated by arrows, such that arrows directed toward the root indicate influx and arrows directed away from the root denote efflux. Scaling bars correspond to the distance along the root and the flux magnitude. Microelectrodes were vibrated perpendicularly to the root with an amplitude of 30 μm such that the extremes of the vibration were between 30 and 60 μm from the root surface.
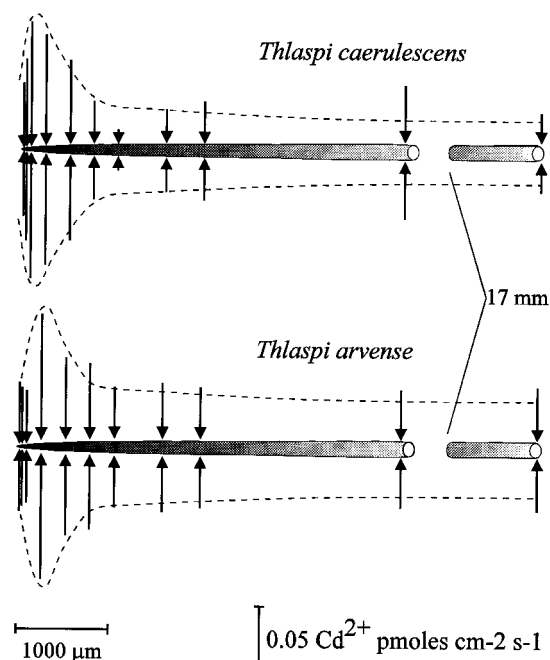

Figure 7. Diagram illustrating the Cd^{2+} flux profile along a single root of the Zn/Cd hyperaccumulator *T. caerulescens* and the nonaccumulator *T. arvense*. Seedlings were exposed overnight to the 50 μM Ca(NO$_3$)$_2$ plus 5 μM Cd(NO$_3$)$_2$ solution. Flux measurements were carried out in 50 μM Ca(NO$_3$)$_2$ plus 5 μM Cd(NO$_3$)$_2$ at different positions along the root. The position and the magnitude of the fluxes are indicated by arrows, such that arrows directed toward the root indicate influx and arrows directed away from the root denote efflux. Scaling bars correspond to the distance along the root and the flux magnitude. Microelectrodes were vibrated perpendicularly to the root with an amplitude of 30 μm, such that the extremes of the vibration were between 30 and 60 μm from the root surface.

logical systems. To our knowledge, this is the first report of the use of Cd^{2+}-selective microelectrodes for any biological application. The ionophore cocktail provides a highly sensitive Cd^{2+} electrode over a wide range of activities, with a Cd^{2+} detection limit (in simple Cd^{2+} solutions) below 1 μM (Fig. 1). Thus, the electrode remains highly sensitive to Cd^{2+} in the range of activities that are relevant to ion transport in plants growing on heavy-metal-contaminated soils (Brown et al., 1994; Jopony and Young, 1994).

Complications from potentially interfering cations were assessed using a variety of techniques and found to be minimal. The addition of Ca^{2+} to the experimental solutions had negligible effects on the response of the microelectrode (Fig. 2). Moreover, this electrode showed a high sensitivity when calibrated in an "artificial cytoplasm solution" (Fig. 3), despite the very high K^+ and Mg^{2+} activities in the test medium. The slopes of the calibration curves obtained under different ionic conditions were Nernstian and indicate that this type of electrode system can be used to estimate intracellular Cd^{2+} activities. Furthermore, the electrode was shown to be pH insensitive (Fig. 4), further supporting its usefulness in intracellular and extracellular applications. Estimates of intracellular ion activities using ISEs, taking into account total ion in-

terference, have been extensively reviewed (Steiner et al., 1979; Croxton and Armstrong, 1992). The development of this Cd^{2+} microelectrode will allow us to simultaneously monitor the uptake and accumulation of Cd^{2+} into plant roots, allowing for detailed studies into the mechanism and regulation of Cd^{2+} uptake into roots and other plant tissues.

A number of techniques were used to assess the electrode sensitivity for Cd^{2+} in the presence of other interfering cations. In the case of the MPM, we found that only Pb^{2+} and Cu^{2+} influenced the electrical output of the electrode. Other interfering ions tested had no direct effect on the electrode's output. It was possible to only crudely estimate the selectivity of the electrode for Cd^{2+} over other interfering cations using the MPM. From the data we can estimate that the electrode was between 250 and 500 times more selective for Cd^{2+} over other cations. The selectivity values calculated by the MPM are specific to the experimental conditions (Bakker, 1997a) imposed on the test solution. These MPM-selectivity coefficients should only serve as an indication of an ion's potential to be an interferent. We were able to calculate more general selectivity coefficients using the technique of Bakker (1996, 1997a, 1997b), which involved preconditioning the electrode in a solution containing the interfering cation prior to any Cd^{2+} exposure. The selectivity coefficients calculated using this technique confirm that there is minimal interference by any of the 11 divalent and monovalent cations tested (Table I). In fact, our Cd^{2+} microelectrode exhibited a greater Cd^{2+} selectivity than was previously reported when the ionophore was first synthesized (Schneider et al., 1980). This lack of interference is an important requirement for the measurement of Cd^{2+} fluxes along the root. If other cations interfere with the operation of the electrode and their fluxes are substantial, then the operation of the system and the ease of measurement would be compromised. In addition, the ability of the system to operate in the presence of other cations without interference allows for studies in which the competitive aspects of uptake can be assessed.

The vibrating microelectrode system provides the advantages of having a high degree of both spatial and temporal resolution. The system is capable of measuring very small Cd^{2+} gradients, as well as measuring fluxes at specific locations along the root. We were able to measure Cd^{2+} fluxes in both wheat and *T. caerulescens* and *T. arvense* roots. The flux profile observed along the roots had a distinct spatial organization, with a much higher Cd^{2+} influx in the few first millimeters back from the root apex and significantly smaller fluxes in the root zones behind this apical region. Similar flux profiles have been reported for Ca^{2+} and Mg^{2+} fluxes. Ryan et al. (1990) found no significant Ca^{2+} influxes beyond 3 mm back from the maize root apex. Huang et al. (1992a) found that Ca^{2+} influx measured 1 and 2 mm back from the root apex was 4 times larger than Ca^{2+} uptake measured farther back from the root apex, although the Ca^{2+} influx in the root cap and meristem region of wheat roots was smaller than the Ca^{2+} flux entering the root just behind this region. Grunes et al. (1993) found an identical spatial pattern for Mg^{2+} influx along wheat roots. Likewise, Ca^{2+} influx into *Limnobium stoloniferum* root

hairs was found to be localized to the root hair apex (Jones et al., 1995). Our preliminary results indicate that there was no difference in either the magnitude or the spatial aspects of the Cd^{2+} flux profile among the two species of *Thlaspi* that we tested. This is despite the fact that these two species have been shown to vary in the tolerance and accumulation of both Cd^{2+} and Zn^{2+}.

Previous studies (Vasquez et al., 1992; Brown et al., 1995) have demonstrated that *T. caerulescens* can accumulate significant levels of Cd in both roots and shoots. Perhaps differences between these two species would have been noted had the experiments been carried out over a much longer time. Cd^{2+} fluxes were not observed until the root system was exposed overnight to a solution containing Cd^{2+}, suggesting that some type of transport "activation" is induced by the presence of the ion. Such observations encourage research characterizing Cd^{2+} fluxes from the two *Thlaspi* spp. grown under different nutrient regimens, as well as measuring intracellular Cd^{2+} activities in root and leaf cells. Investigators have also shown that *Brassica juncea*, a high-biomass crop plant, can accumulate substantial amounts of Cd in its shoots and roots (Salt et al., 1995). A comparison of Cd^{2+} uptake in the roots of the two *Thlaspi* spp. and of *Brassica juncea* would also be quite interesting. All of these studies are now possible given the development of a highly sensitive Cd^{2+}-selective microelectrode. Indeed, it should be a useful tool to further our understanding of the physiology of heavy-metal uptake and accumulation in plants.

LITERATURE CITED

Baker AJM, Reeves RD, Hajar ASM (1994) Heavy metal accumulation and tolerance in British populations of the metallophyte *Thlaspi caerulescens* J & c Presl (Brasssicaceae). New Phytol **127:** 61–68

Bakker E (1996) Determination of improved selectivity coefficients of polymer membrane ion-selective electrodes by conditioning with a discriminated ion. J Electrochem Soc **143:** L83–L85

Bakker E (1997a) Selectivity of liquid membrane ion-selective electrodes. Electroanalysis **9:** 7–12

Bakker E (1997b) Determination of unbiased selectivity coefficients of neutral carrier-based cation-selective electrodes. Anal Chem **69:** 1061–1069

Brooks RR, Lee J, Reeves R, Jaffré T (1977) Detection of nickelferous rocks by analysis of herbarium specimens of indicator plants. J Geochem Explor **7:** 49–58

Brown SL, Chaney RL, Angle JS, Baker AJM (1994) Phytoremediation potential of *Thlaspi caerulescens* and bladder campion for zinc- and cadmium-contaminated soils. J Environ Qual **23:** 1151–1157

Brown SL, Chaney RL, Angle JS, Baker AJM (1995) Zinc and cadmium uptake by hyperaccumulator *Thlaspi caerulescens* grown in nutrient solution. Soil Sci Soc Am J **59:** 125–133

Buck RP, Lindner E (1994) Recommendations for nomenclature of ion-selective electrodes. Pure Appl Chem **66:** 2527–2536

Cataldo D, Garland TR, Wildung RE (1983) Cadmium uptake in intact soybean plants. Plant Physiol **73:** 844–848

Chaney RL (1993) Zinc phytotoxicity. *In* AD Robson, ed, Zinc in Soil and Plants. Kluwer Academic Publishers, Dordrecht, The Netherlands, pp 135–150

Croxton TL, Armstrong WM (1992) Calibration of ion-selective microelectrodes. Am J Physiol **262:** C1324–C1334

Gadzekpo VPY, Christian GD (1984) Determination of selectivity coefficients of ion-selective electrodes by a matched potential method. Anal Chim Acta **164:** 279–282

Grunes DL, Ohno T, Huang JW, Kochian LV (1993) Effects of aluminum on magnesium, calcium, and potassium in wheat forages. S Golf, D Dralle, L Vecchiet, eds, Magnesium 1993. John Libbey & Co., London, pp 79–88

Henriksen G, Bloom AJ, Spanswick RM (1990) Measurement of net fluxes of ammonium and nitrate at the surface of barley roots using ion-selective microelectrodes. Plant Physiol **93:** 271–280

Henriksen G, Raman DR, Walker LP, Spanswick RM (1992) Measurement of net fluxes of ammonium and nitrate at the surface of barley roots using ion specific microelectrodes. II. Patterns of uptake along the root axis and evaluation of the microelectrode flux estimation technique. Plant Physiol **99:** 734–747

Huang JW, Grunes DL, Kochian LV (1992a) Aluminum effects on the kinetics of calcium uptake into cells of the wheat root apex. Planta **188:** 414–421

Huang JW, Shaff JE, Grunes DL, Kochian LV (1992b) Aluminum effects on calcium fluxes at the root apex of aluminum-tolerant and aluminum-sensitive wheat cultivars. Plant Physiol **98:** 230–237

Jones DL, Shaff JE, Kochian LV (1995) Role of calcium and other ions in directing root hair tip growth in *Limnobium stoloniferum*. I. Inhibition of tip growth by aluminum. Planta **197:** 672–680

Jopony M, Young SD (1994) The solid-solution equilibria of lead and cadmium in polluted soils. Eur J Soil Sci **45:** 59–70

Kochian LV, Shaff JE, Kuhtreiber WM, Jaffe LF, Lucas W (1992) Use of an extracellular, ion-selective, vibrating microelectrode system for the quantification of K^+, H^+, and Ca^{2+} fluxes in maize roots and maize suspension cells. Planta **188:** 601–610

Kochian LV, Shaff JE, Lucas W (1989) High affinity K^+ uptake in maize roots. A lack of coupling with H^+ efflux. Plant Physiol **91:** 1202–1211

Kühtreiber WM, Jaffe LF (1990) Detection of extracellular calcium gradients with a calcium-specific vibrating electrode. J Cell Biol **110:** 1565–1573

Lasat MM, Baker AJM, Kochian LV (1996) Physiological characterization of root Zn^{2+} absorption and translocation to shoots in Zn hyperaccumulator and nonaccumulator species of *Thlaspi*. Plant Physiol **112:** 1715–1722

Lucas WJ, Kochian LV (1986) Ion transport processes in corn roots: an approach utilizing microelectrode techniques. *In* WG Gensler, ed, Advanced Agricultural Instrumentation: Design and Use. Martinus Nijhoff Publishers, Boston, MA, pp 402–425

McClure PR, Kochian LV, Spanswick RM, Shaff JE (1990) Evidence for cotransport of nitrate and protons in maize roots. II. Measurements of NO_3^- and H^+ fluxes with ion-selective microelectrodes. Plant Physiol **93:** 290–294

Miyasaka SC, Kochian LV, Shaff JE, Foy CD (1989) Mechanisms of aluminum tolerance in wheat. An investigation of genotypic differences in rhizosphere pH, K^+, and H^+ transport, and root-cell membrane potentials. Plant Physiol **96:** 737–743

Mullins GL, Sommers LE (1986) Cadmium and zinc influx characteristics by intact corn (*Zea mays* L.) seedlings. Plant Soil **96:** 153–164

Newman IA, Kochian LV, Grusak MA, Lucas WA (1987) Fluxes of H^+ and K^+ in corn roots. Characterization and stoichiometries using ion-selective microelectrodes. Plant Physiol **84:** 1177–1184

Parker DR, Norvell WA, Chaney RL (1995) GEOCHEM-PC: a chemical speciation program for IBM and compatible computers. *In* RH Loeppert, AP Schwab, Goldberg S, eds, Chemical Equilibrium and Reaction Models. Soil Science Society of America, Madison, WI, pp 253–269

Parsons R (1959) Handbook of Electrochemical Constants. Buttersworth Scientific Publications, London, pp 78–79

Ryan PR, Kochian LV (1993) Interaction between aluminum toxicity and calcium uptake at the root apex of near-isogenic lines of wheat (*Triticum aestivum* L.) differing in aluminum tolerance. Plant Physiol **102:** 975–982

Ryan PR, Newman IA, Shields B (1990) Ion fluxes in corn roots measured by microelectrodes with ion-specific liquid membranes. J Membr Sci **53:** 59–69

Ryan PR, Shaff, JE, Kochian LV (1992) Aluminum toxicity in roots. Correlation among ionic currents, ion fluxes, and root elongation in aluminum-sensitive and aluminum-tolerant wheat cultivars. Plant Physiol **99:** 1193–1200

Salt DE, Prince RC, Pickering IJ, Raskin I (1995) Mechanisms of cadmium mobility and accumulation in Indian mustard. Plant Physiol **109:** 1427–1433

Schneider JK, Hofstetter P, Pretsch E, Amman D, Simon W (1980) *N,N,N',N'*-Tetrabutyl-3,6-dioxaoctan-dithioamid, ionophor mit selektivität für Cd^{2+}. Helv Chim Acta **63:** 217–224

Smith PJS, Sanger RH, Jaffe LF (1994) The vibrating Ca^{2+} electrode: a new technique for detecting plasma membrane regions of Ca^{2+} influx and efflux. Methods Cell Biol **40:** 115–134

Steiner RA, Oehme M, Ammann D, Simon W (1979) Neutral carrier sodium ion-selective microelectrode for intracellular studies. Anal Chem **51:** 351–353

Umezawa Y, Umezawa K, Sato H (1995) Selectivity coefficients for ion-selective electrodes: recommended methods for reporting $K^{pot}_{A,B}$ values. Pure Appl Chem **67:** 507–518

Vasquez MD, Barceló J, Poschenreider Ch, Mádico J, Hatton P, Baker AJM, Cope GH (1992) Localization of zinc and cadmium in *Thlaspi caerulescens* (Brassicaceae) that can hyperaccumulate both metals. J Plant Physiol **140:** 350–355